Charged-particle pseudorapidity distributions in Au+Au collisions at RHIC*

WANG Zeng-Wei(王增伟)[1)] JIANG Zhi-Jin(姜志进)[2)]

(Science College, Shanghai Science and Technology University, Shanghai 200093, China)

Abstract Using the Glauber model, we present the formulas for calculating the numbers of participants, spectators and binary nucleon-nucleon collisions. Based on this work, we get the pseudorapidity distributions of charged particles as the function of the impact parameter in nucleus-nucleus collisions. The theoretical results agree well with the experimental observations made by the BRAHMS Collaboration in Au+Au collisions at $\sqrt{s_{\rm NN}}$=200 GeV in different centrality bins over the whole pseudorapidity range.

Key words pseudorapidity distribution, Glauber model, binary nucleon-nucleon collision, spectator

PACS 25.75.Dw

1 Introduction

Nucleus-nucleus collisions from the Relativistic Heavy Ion Collider (RHIC) at the Brookhaven National Laboratory (BNL) offer an opportunity to study the strongly interacting matter in the laboratory. RHIC was built to search for quark matter, or the so-called quark-gluon plasma (QGP). The charged-particle pseudorapidity distribution $\mathrm{d}N_{AB}/\mathrm{d}\eta$ is one of the first measurements made at RHIC. It contains a lot of information about the hot and dense matter produced in collisions[1—5] at the initial time, hence it forms one of the most important observables for exploring QGP. The distribution of $\mathrm{d}N_{AB}/\mathrm{d}\eta$ over the entire range of pseudorapidity η represents a time-integral of particle production throughout the collision. It reflects all effects that contribute to the production of charged particles. In addition to the influence of both hard and soft production processes, it is sensitive to nuclear effects in the initial parton distributions, as well as to effects from hadronic re-interactions in the final state[6]. Therefore, the distribution of $\mathrm{d}N_{AB}/\mathrm{d}\eta$ provides us with a feasible means for understanding the mechanism of particle generation and interaction in the final state.

Since the first run of RHIC in 2000, a great deal of data have been accumulated and a comprehensive analysis of these data has been carried out. The experimental data about the charged-particle pseudorapidity distributions in Au+Au collisions have been presented by the PHOBOS Collaboration[7], the PHENIX Collaboration[8], and the BRAHMS Collaboration[9]. All these results show that, for different centrality bins, the shapes and ranges of pseudorapidity distributions are approximately the same. But their heights decrease evidently (especially in the central pseudorapidity region) with the increase of centralities.

Ref. [10] has discussed the observed phenomena by employing the overlapping cylinder model, which is developed out of the thermalized cylinder model[11—15]. With the help of event generator PYTHIA, Ref. [1] has also investigated the same experimental observations by virtue of the quark combination model. In our recent work[16], by making use of repeated additions of rapidity distributions in binary nucleon-nucleon collisions, we have got the distribution of $\mathrm{d}N_{AB}/\mathrm{d}\eta$ as the function of the impact parameter in nucleus-nucleus collisions. The theoretical model gives a good description to the experimental data in the central pseudorapidity region for different

Received 15 July 2008

* Supported by Key Foundation of Shanghai (S30501)

1) E-mail: wzwei@126.com

2) E-mail: jzj265@163.com

centrality bins. However, in the large pseudorapidity region, our calculations are somewhat lower than the data.

In this article, on the basis of the Glauber model[17, 18], we first present the formulas for determining the number of participants, spectators and binary nucleon-nucleon collisions in heavy-ion collisions. These numbers are then used to constitute the function form of $\mathrm{d}N_{AB}/\mathrm{d}\eta$, which is impact parameter dependent and will have a comparison with the experimental measurements made by the BRAHMS Collaboration in different centrality Au+Au collisions at $\sqrt{s_{\mathrm{NN}}}$=200 GeV.

2 The number of participants, spectators and binary nucleon-nucleon collisions in heavy-ion collisions

2.1 The number of participants and spectators

The nucleons in the nucleus obey Wood-Saxon distribution

$$\rho(r)=\frac{\rho_0}{1+\exp[(r-r_0)/a]}\ , \tag{1}$$

where $r_0=1.19A^{1/3}-1.61A^{-1/3}$, $a=0.54$ fm[19, 20], A is the mass number of the nucleus. ρ_0 in Eq. (1) is determined by $\int_V \rho(r)\mathrm{d}V=A$. For nucleus Au, $A=197$, so $r_0=6.65$ fm, $\rho_0=0.15046/\mathrm{fm}^3$. Fig. 1 shows the relation between nuclear density $\rho(r)$ and radius r of Au.

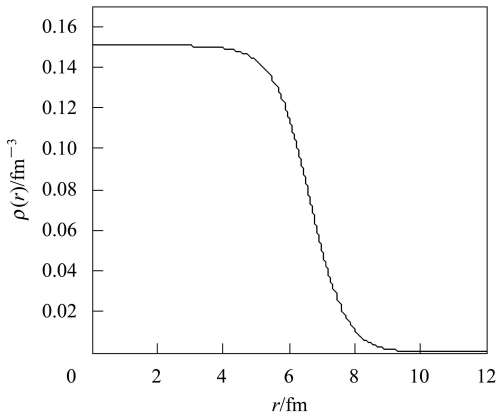

Fig. 1. The relation between nuclear density $\rho(r)$ and radius r of Au.

From this figure we can see that nucleons in Au are mainly gathered at the range of $r\leqslant 5$ fm. Beyond this range, the number of nucleons decreases rapidly and while $r>10$ fm, there are nearly no nucleons. So in the following calculation, we will take r=10 fm.

From nuclear density $\rho(r)$, we have the nuclear thickness function

$$T(\boldsymbol{s})=\int\rho(\boldsymbol{s},z)\mathrm{d}z\ . \tag{2}$$

It is the number of nucleons in the flux tube which possesses the unit bottom area and locates at the displacement $\boldsymbol{s}$ relative to the center of the nucleus (cf. Fig. 2).

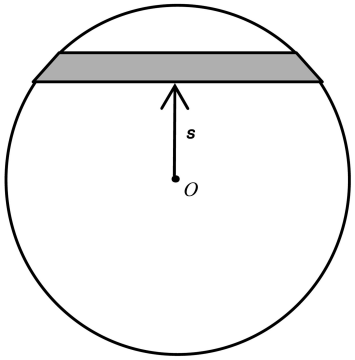

Fig. 2. The flux tube with the unit bottom area located at the displacement $\boldsymbol{s}$ with respect to the center of the nucleus.

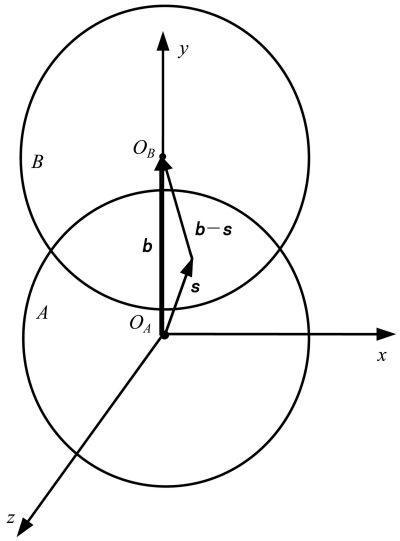

Fig. 3. An A—B nucleus collision with impact parameter $\boldsymbol{b}$.

Considering the collision between the A—B nucleus with impact parameter $\boldsymbol{b}$, see Fig. 3. If the total inelastic nucleon-nucleon cross section is taken to be $\sigma_{\mathrm{NN}}^{\mathrm{in}}$, then $\sigma_{\mathrm{NN}}^{\mathrm{in}}T_B(\boldsymbol{s}-\boldsymbol{b})$ is the number of nucleons that a nucleon in nucleus A at position $\boldsymbol{s}$ will encounter as it passes through nucleus B. As can be seen from Fig. 3, $\boldsymbol{s}$ is the function of x and y, and the length of it is

$$s(x,y)=\sqrt{x^2+y^2}\ .$$

The probability of that nucleon surviving the collisions is $\exp[-\sigma_{\rm NN}^{\rm in}T_B(\boldsymbol{s}-\boldsymbol{b})]$, and the probability suffering the collisions is $1-\exp[-\sigma_{\rm NN}^{\rm in}T_B(\boldsymbol{s}-\boldsymbol{b})]$.

Hence, for nucleus A, the number of participants in the flux tube (Fig. 2) at position $\boldsymbol{s}$ (Fig. 3) is

$$n_A(\boldsymbol{b},\boldsymbol{s})=T_A(\boldsymbol{s})\{1-\exp[-\sigma_{\rm NN}^{\rm in}T_B(\boldsymbol{s}-\boldsymbol{b})]\}. \quad (3)$$

Similarly, for nucleus B, the number of participants in the same flux tube is

$$n_B(\boldsymbol{b},\boldsymbol{s})=T_B(\boldsymbol{s}-\boldsymbol{b})\{1-\exp[-\sigma_{\rm NN}^{\rm in}T_A(\boldsymbol{s})]\}, \quad (4)$$

and

$$\begin{aligned} n_{\rm Part}(\boldsymbol{b},\boldsymbol{s}) \;=\; & n_A(\boldsymbol{b},\boldsymbol{s})+n_B(\boldsymbol{b},\boldsymbol{s})= \\ & T_A(\boldsymbol{s})\{1-\exp[-\sigma_{\rm NN}^{\rm in}T_B(\boldsymbol{s}-\boldsymbol{b})]\}+ \\ & T_B(\boldsymbol{s}-\boldsymbol{b})\{1-\exp[-\sigma_{\rm NN}^{\rm in}T_A(\boldsymbol{s})]\}, \quad (5) \end{aligned}$$

is the total participants in the concerned flux tube. Thus the number of participants in an A—B nucleus collision with impact parameter $\boldsymbol{b}$ is

$$N_{\rm Part}(b)=\int_{-\sqrt{r^2-\frac{\boldsymbol{b}^2}{4}}}^{\sqrt{r^2-\frac{\boldsymbol{b}^2}{4}}}{\rm d}x\int_{\boldsymbol{b}-\sqrt{r^2-x^2}}^{\sqrt{r^2-x^2}}n_{\rm Part}(\boldsymbol{b},\boldsymbol{s}){\rm d}y\ , \quad (6)$$

where r is the radius of Au, and for equal-nucleus collisions, the number of spectators of each nucleus in the collision region is

$$N_{\rm Spec}(\boldsymbol{b})=N_{\rm Total}(\boldsymbol{b})-\frac{N_{\rm Part}(\boldsymbol{b})}{2}\ , \quad (7)$$

where $N_{\rm Total}(\boldsymbol{b})$ stands for the total number of nucleons of each nucleus in the collision region. For a certain centrality collision, the mean number of total nucleons, participants or spectators can be obtained from equation

$$\bar{N}=\frac{\int N(\boldsymbol{b}){\rm d}^2\boldsymbol{b}}{\int{\rm d}^2\boldsymbol{b}}\ . \quad (8)$$

As far as an undeformed or isotropic nucleus is concerned, quantities with $\boldsymbol{b}$ as variable depend only on the size of $\boldsymbol{b}$, but are independent of its direction, such as $N_{\rm Part}(\boldsymbol{b})=N_{\rm Part}(b)$. In this paper, we will only discuss this simple case.

Table 1. The range of impact parameter $\boldsymbol{b}$, the numbers of $\bar{N}_{\rm Total}$, $\bar{N}_{\rm Part}$ and $\bar{N}_{\rm Spec}$ in different centrality Au+Au collisions at $\sqrt{s_{\rm NN}}$=200 GeV. The numbers inside parentheses are the results given by the BRAHMS Collaboration[9].

centrality bins	b/fm	$\bar{N}_{\rm Total}$	$\bar{N}_{\rm Part}$	$\bar{N}_{\rm Spec}$	$\bar{N}_{\rm NN}$
0—5%	0—3.31	195.81	347.3(357±8)	22.16	1018.3(1000±125)
5%—10%	3.31—4.69	189.08	293.3(306±11)	42.43	810.9(785±115)
10%—20%	4.69—6.63	168.63	231.2(239±10)	53.03	586.1(552±100)
20%—30%	6.63—8.12	138.48	163.6(168±9)	56.68	372.7(335±58)
30%—40%	8.12—9.37	110.72	113.9(114±9)	53.77	228.4(192±43)
40%—50%	9.37—10.48	86.50	76.0(73±8)	48.50	131.9(103±31)

Table 1 presents the range of impact parameter b, the mean numbers of $\bar{N}_{\rm Total}$, $\bar{N}_{\rm Part}$ and $\bar{N}_{\rm Spec}$ in different centrality Au+Au collisions at $\sqrt{s_{\rm NN}}=200$ GeV. In calculations we take $\sigma_{\rm NN}^{\rm in}$=42 mb[21], and the centrality bins are defined as the percentages of the total inelastic cross section $\sigma_{\rm AuAu}^{\rm in}$=6.9 b. The values inside the parentheses are the results given by the BRAHMS Collaboration[9]. From Table 1 we can see that the calculations from Eq. (6) and (8) are in good agreement with the results from the BRAHMS Collaboration.

2.2 The number of binary nucleon-nucleon collisions

To get the number of binary nucleon-nucleon collisions, dividing Eq. (1) by nuclear mass number A, we have

$$\rho_{\rm P}(r)=\frac{\rho_0}{A\{1+\exp[(r-r_0)/a]\}}\ . \quad (9)$$

The meaning of which is the probability for finding a nucleon in unit volume. From $\rho_{\rm P}(r)$, we have another kind of nuclear thickness function

$$T_{\rm P}(s)=\int\rho_{\rm P}(\boldsymbol{s},z){\rm d}z\ , \quad (10)$$

which is the probability for finding a nucleon in the flux tube as shown in Fig. 2. Hence, in an A—B nucleus collision with impact parameter $\boldsymbol{b}$, the probability for having a binary nucleon-nucleon collision in a unit cross section is

$$T_{\rm P}(\boldsymbol{b})=\int T_{{\rm P}A}(\boldsymbol{s})T_{{\rm P}B}(\boldsymbol{s}-\boldsymbol{b}){\rm d}^2\boldsymbol{s}\ , \quad (11)$$

where the vector $\boldsymbol{s}$ is the same as that in Fig. 3. The probability for having n times of binary nucleon-

nucleon collisions is

$$P(n,\boldsymbol{b})=\begin{pmatrix} AB \\ n \end{pmatrix}\left[T_{\rm P}(\boldsymbol{b})\sigma_{\rm NN}^{\rm in}\right]^n\left[1-T_{\rm P}(\boldsymbol{b})\sigma_{\rm NN}^{\rm in}\right]^{AB-n}\ , \tag{12}$$

which certainly meets the condition of normalization

$$\sum_{n=0}^{AB}P(n,\boldsymbol{b})=1\ . \tag{13}$$

The number of binary nucleon-nucleon inelastic collisions in an A—B nucleus collision at impact parameter $\boldsymbol{b}$ can then be written as

$$N_{\rm NN}(\boldsymbol{b})=\frac{\sum\limits_{n=1}^{AB}nP(n,\boldsymbol{b})}{\sum\limits_{n=1}^{AB}P(n,\boldsymbol{b})}\ . \tag{14}$$

Known from Eq. (12),

$$\sum_{n=1}^{AB}nP(n,\boldsymbol{b})=ABT_{\rm P}(\boldsymbol{b})\sigma_{\rm NN}^{\rm in}\ . \tag{15}$$

Inserting Eqs. (13) and (15) into Eq. (14), it becomes

$$N_{\rm NN}(\boldsymbol{b})=\frac{ABT_{\rm P}(\boldsymbol{b})\sigma_{\rm NN}^{\rm in}}{1-[1-T_{\rm P}(\boldsymbol{b})\sigma_{\rm NN}^{\rm in}]^{AB}}\ . \tag{16}$$

Replacing $N(\boldsymbol{b})$ in Eq. (8) by $N_{\rm NN}(\boldsymbol{b})$, we can get the mean number of binary nucleon-nucleon inelastic collisions $\bar{N}_{\rm NN}$ for a certain centrality bin. Table 1 shows $\bar{N}_{\rm NN}$ in each centrality Au+Au collision at $\sqrt{s_{\rm NN}}$=200 GeV. The numbers inside the parentheses are the results given by the BRAHMS Collaboration. From this table we can see that the calculations from Eq. (8) and (16) are very consistent with the results from the BRAHMS Collaboration.

3 Charged-particle pseudorapidity distributions in heavy-ion collisions

3.1 Charged-particle pseudorapidity distributions in nucleon-nucleon collisions

For the sake of utilizing later, we will first say some things about the charged-particle pseudorapidity distributions in nucleon-nucleon collisions.

The charged particles generated in a nucleon-nucleon collision arise from two ways. One is the lost energy in collisions; the other one is two leading particles. Known from Ref. [22], the pseudorapidity distribution of charged particles in nucleon-nucleon collisions can be written as

$$\frac{{\rm d}N_{\rm NN}(\sqrt{s_{\rm NN}})}{{\rm d}y}=\frac{C(\sqrt{s_{\rm NN}})}{1+\exp\left[\dfrac{|y|-y_0(\sqrt{s_{\rm NN}})}{\Delta}\right]}\ , \tag{17}$$

where Δ is the constant affecting the width of distribution, $C(\sqrt{s_{\rm NN}})$ is a $\sqrt{s_{\rm NN}}$ dependent function determining the height of distribution, and $y_0(\sqrt{s_{\rm NN}})$ is another $\sqrt{s_{\rm NN}}$ dependent function fixing the peak positions of distribution. In this paper we take them to be

$$\Delta=0.7,$$

$$C(\sqrt{s_{\rm NN}})=0.525\ln\sqrt{s_{\rm NN}}+0.02\ ,$$

$$y_0(\sqrt{s_{\rm NN}})=0.42\ln\sqrt{s_{\rm NN}}+1.4\ .$$

The relation between rapidity and pseudorapidity is

$$y=\frac{1}{2}\ln\left[\frac{\sqrt{p_{\rm T}^2\cosh^2\eta+m^2}+p_{\rm T}\sinh\eta}{\sqrt{p_{\rm T}^2\cosh^2\eta+m^2}-p_{\rm T}\sinh\eta}\right], \tag{18}$$

and the relation between pseudorapidity and rapidity distribution is

$$\frac{{\rm d}N_{\rm NN}(\sqrt{s_{\rm NN}})}{{\rm d}\eta}=\sqrt{1-\frac{m^2}{m_{\rm T}^2\cosh^2 y}}\frac{{\rm d}N_{\rm NN}(\sqrt{s_{\rm NN}})}{{\rm d}y}\ . \tag{19}$$

Figure 4 shows the charged-particle pseudorapidity distributions in p+p collisions at $\sqrt{s_{\rm NN}}$=200 GeV. The stars are the experimental results measured by the UA5 Collaboration[23]. The solid curve is the result from Eq. (19). From this figure we can see that Eq. (17) gives a good description for the experimental measurements.

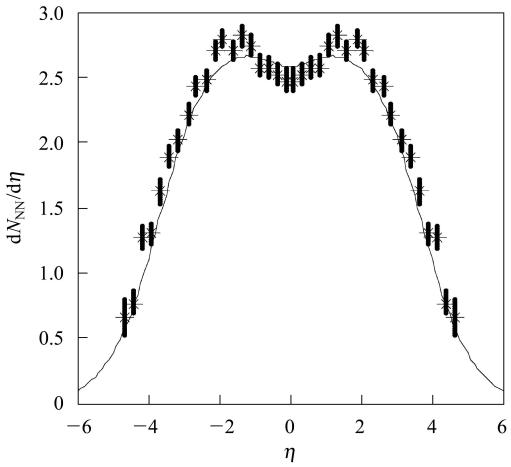

Fig. 4. The charged-particle pseudorapidity distributions in p+p collisions at $\sqrt{s_{\rm NN}}$ = 200 GeV. The stars are the experimental measurements made by the UA5 Collaboration[23]. The solid curve is the result from Eq. (19).

3.2 Charged-particle pseudorapidity distributions in heavy-ion collisions

In nucleus-nucleus collisions, the energy of a nucleon will become less and less along with its collisions with other nucleons. The lost energy is accumulated

in the region around the center of mass and is finally frozen into the measurable charged particles in the final state. It is obvious that the charged particles produced in a nucleus-nucleus collision come from three channels. One is the lost energy; the other one is the leading particles and the third one is the spectators. As mentioned above, the first two channels may be attributed to binary nucleon-nucleon collisions. Hence, in nucleus-nucleus collisions, the charged-particle pseudorapidity distributions may be divided into two parts. One is from binary nucleon-nucleon collisions; the other one is from spectators.

3.2.1 Charged-particle pseudorapidity distributions from binary nucleon-nucleon collisions

In an A—B nucleus collision at impact parameter $\boldsymbol{b}$, the rapidity distribution of charged particles produced in binary nucleon-nucleon collisions can be expressed as

$$\frac{\mathrm{d}N_{AB}^{\mathrm{Bina}}(\boldsymbol{b})}{\mathrm{d}y}=\sum_{n=1}^{AB}P(n,\boldsymbol{b})\sum_{i=1}^{n}\frac{\mathrm{d}N_{\mathrm{NN}}(\sqrt{s_{\mathrm{NN}}^{i}},\boldsymbol{b})}{\mathrm{d}y}\ , \quad (20)$$

where $P(n,\boldsymbol{b})$, given by Eq. (12), is the probability for the occurrence of n times of binary nucleon-nucleon collisions. $\mathrm{d}N_{\mathrm{NN}}(\sqrt{s_{\mathrm{NN}}^{i}},\boldsymbol{b})/\mathrm{d}y$ is the rapidity distribution in binary nucleon-nucleon collision with c.m.s. energy of $\sqrt{s_{\mathrm{NN}}^{i}}$. In this paper, it is taken to have the form as in Eq. (17). This means that the contributions from both the lost energy and leading particles are all included in binary nucleon-nucleon collisions. Moreover, it is worth while pointing out that the transverse momentum of the charged particles in the final state increases as the impact parameter $\boldsymbol{b}$ decreases[24—26]. Thus, in Eq. (20), the rapidity distribution in binary nucleon-nucleon collisions depends on the impact parameter $\boldsymbol{b}$ of nucleus-nucleus collisions.

In order to get the distribution of $\mathrm{d}N_{AB}^{\mathrm{Bina}}(\boldsymbol{b})/\mathrm{d}y$ from Eq. (20), we should know the c.m.s. energy in each binary nucleon-nucleon collision. This is impossible in fact. Here we will take a simple way to deal with Eq. (20).

As the first step of simplification, we may ignore the differences in c.m.s. energy for different binary nucleon-nucleon collisions. For example, in Au+Au collisions at $\sqrt{s_{\mathrm{NN}}}=200$ GeV, we may just take $\sqrt{s_{\mathrm{NN}}^{i}}=\sqrt{s_{\mathrm{NN}}}=200$ GeV for all binary nucleon-nucleon collisions. Then, from Eq. (15) and (16), Eq. (20) becomes

$$\frac{\mathrm{d}N_{AB}^{\mathrm{Bina}}(\boldsymbol{b})}{\mathrm{d}y}\approx N_{\mathrm{NN}}(\boldsymbol{b})\left\{1-[1-T_{\mathrm{P}}(\boldsymbol{b})\sigma_{\mathrm{NN}}^{\mathrm{in}}]^{AB}\right\}\times\frac{\mathrm{d}N_{\mathrm{NN}}(\sqrt{s_{\mathrm{NN}}},\boldsymbol{b})}{\mathrm{d}y}\ , \quad (21)$$

where, $T_{\mathrm{P}}(\boldsymbol{b})$ and $N_{\mathrm{NN}}(\boldsymbol{b})$ are given by Eq. (11) and (16), separately. However, the fact is that the c.m.s. energy in different binary nucleon-nucleon collisions is different. The smaller the impact parameter, the larger is the number of $N_{\mathrm{NN}}(\boldsymbol{b})$ (see Table 1). Then, the less the mean c.m.s. energy is for each binary nucleon-nucleon collision due to more energy loss in more times of collisions. Hence, the smaller the contribution is to the yield of charged particles. Accordingly, from this sense, $\mathrm{d}N_{AB}(\boldsymbol{b})/\mathrm{d}y$ should decrease with $N_{\mathrm{NN}}(\boldsymbol{b})$. Thus, we introduce the factor of energy loss $\beta(\boldsymbol{b})$, which is defined as

$$\beta(\boldsymbol{b})=1+\alpha(\boldsymbol{b})[N_{\mathrm{NN}}(\boldsymbol{b})-1], \quad (22)$$

where $\alpha(\boldsymbol{b})$ is a free parameter. Now, as the effect of energy loss is taken into account, Eq. (21) can be rewritten as

$$\frac{\mathrm{d}N_{AB}^{\mathrm{Bina}}(\boldsymbol{b})}{\mathrm{d}y}=\frac{N_{\mathrm{NN}}(\boldsymbol{b})\left\{1-[1-T_{\mathrm{P}}(\boldsymbol{b})\sigma_{\mathrm{NN}}^{\mathrm{in}}]^{AB}\right\}}{\beta(\boldsymbol{b})}\times\frac{\mathrm{d}N_{\mathrm{NN}}(\sqrt{s_{\mathrm{NN}}},\boldsymbol{b})}{\mathrm{d}y}\ . \quad (23)$$

For p+p collision, $N_{\mathrm{NN}}(\boldsymbol{b})=T_{\mathrm{P}}(\boldsymbol{b})\sigma_{\mathrm{NN}}^{\mathrm{in}}=1$ (Eq. (16)), the above equation reduces to the rapidity distribution in the p+p collision. This is just what we expect.

Finally, from Eq. (19), the charged-particle pseudorapidity distribution from the binary nucleon-nucleon collisions is

$$\frac{\mathrm{d}N_{AB}^{\mathrm{Bina}}(\boldsymbol{b})}{\mathrm{d}\eta}=\sqrt{1-\frac{m^{2}}{m_{\mathrm{T}}^{2}(\boldsymbol{b})\cosh^{2}y}}\frac{\mathrm{d}N_{AB}^{\mathrm{Bina}}(\boldsymbol{b})}{\mathrm{d}y}\ . \quad (24)$$

3.2.2 Charged-particle pseudorapidity distributions from spectators

The spectators are those nucleons which do not take part in the collisions as two nuclei penetrate each other. They can be divided into two parts. One is from the region of collision; the other one is from the outside region of collision. Compared with the former, the latter may be ignored, since during the process of nucleus-nucleus collision, the nuclear matter in the outside region of collision is mainly broken into nuclear fragments which make no contribution to the charged particles in the final state. However, the nuclear matter in the collision region is totally split into nucleons due to the violent collisions. Hence, the number of spectators approximately equals the total number of nucleons minus the number of participants in the collision region. Thus we have Eq. (7).

The pseudorapidity distribution of spectators can

be written as

$$\frac{\mathrm{d}N_{AB}^{\mathrm{Spec}}(\boldsymbol{b})}{\mathrm{d}\eta}=\frac{N_{\mathrm{Spec}}(\boldsymbol{b})}{2\cosh^2[\eta-\eta_0(\boldsymbol{b})]}\ , \tag{25}$$

where $\eta_0(\boldsymbol{b})$ is another free parameter determining the central position of distribution. Experimental investigations[27] have shown that $\eta_0(\boldsymbol{b})$ increases with the decrease of $\boldsymbol{b}$. It is obvious that Eq. (25) meets the condition of

$$\int_{-\infty}^{\infty}\frac{\mathrm{d}N_{AB}^{\mathrm{Spec}}(\boldsymbol{b})}{\mathrm{d}\eta}\mathrm{d}\eta=N_{\mathrm{Spec}}(\boldsymbol{b}).$$

3.2.3 Charged-particle pseudorapidity distributions in heavy-ion collisions

From Eqs. (24) and (25), we get the pseudorapidity distributions of charged particles in nucleus-nucleus collisions as

$$\frac{\mathrm{d}N_{AB}(\boldsymbol{b})}{\mathrm{d}\eta}=\frac{\mathrm{d}N_{AB}^{\mathrm{Bina}}(\boldsymbol{b})}{\mathrm{d}\eta}+\frac{\mathrm{d}N_{AB}^{\mathrm{Spec}}(\boldsymbol{b})}{\mathrm{d}\eta}\ . \tag{26}$$

For Au+Au collisions at $\sqrt{s_{\mathrm{NN}}}=200$ GeV, the numerical results of the above equation are shown in Fig. 5. The triangles and circles are the experimental data of the BRAHMS Collaboration[9]; the dotted curves are the results from spectators; the dashed curves are the results from binary nucleon-nucleon collisions; and the solid curves are the sums of dotted and dashed curves. It can be seen from this figure that Eq. (26) fits the experimental data perfectly in each centrality bin over the whole pseudorapidity range. Fig. 5 also shows that the binary nucleon-nucleon collisions are in the predominant position in the distributions.

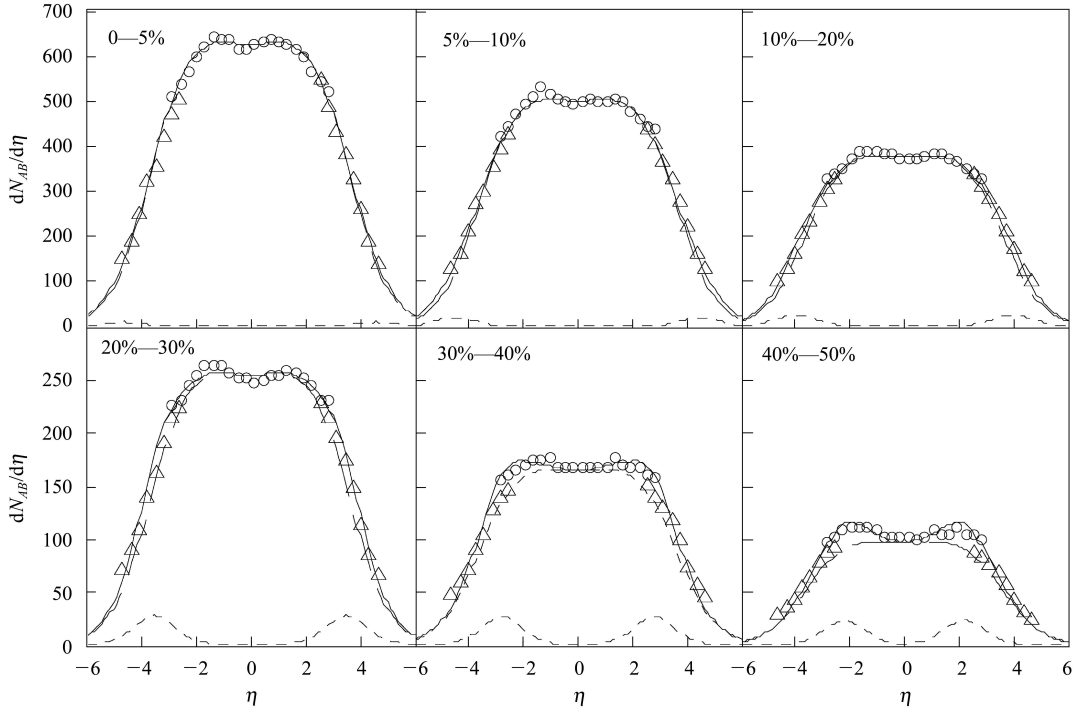

Fig. 5. Charged-particle pseudorapidity distributions in Au+Au collisions at $\sqrt{s_{\mathrm{NN}}}$=200 GeV. The triangles and circles are the experimental data from the BRAHMS Collaboration[9], the dotted curves are the results from spectators; the dashed curves are the results from binary nucleon-nucleon collisions; and the solid curves are the sums of dotted and dashed curves.

In calculations, m in Eq. (18), (19) and (24) is approximately taken to be the mass of π. $p_{\mathrm{T}}(\boldsymbol{b})$ in these equations is obtained from experimental measurements[26]. The free parameters $\alpha(\boldsymbol{b})$ and $\eta_0(\boldsymbol{b})$ are determined by fitting the experimental data. The values of them are summarized in Table 2. This table shows that both $p_{\mathrm{T}}(\boldsymbol{b})$ and $\eta_0(\boldsymbol{b})$ increase with the decrease of $\boldsymbol{b}$. This is consistent with the statements given above. The values of $\alpha(\boldsymbol{b})$ in Table 2 decrease with the decrease of $\boldsymbol{b}$. Substituting them into Eq. (22), we get the variations of $\beta(\boldsymbol{b})$ against centrality bins as shown in Fig. 6. This figure shows that the larger the number of $N_{\mathrm{NN}}(\boldsymbol{b})$, the less the number of charged particles produced in each binary nucleon-nucleon collision (Eq. (23)). This is in accordance with the analysis we made above.

Table 2. The values of $p_{\rm T}(\boldsymbol{b})$, $\alpha(\boldsymbol{b})$, and $\eta_0(\boldsymbol{b})$ in each centrality bin.

centrality bins	$p_{\rm T}(\boldsymbol{b})/({\rm GeV}/c)$	$\alpha(\boldsymbol{b})$	$\eta_0(\boldsymbol{b})$
0—5%	0.450	0.0033	4.6
5%—10%	0.449	0.0041	4.5
10%—20%	0.448	0.0054	4.0
20%—30%	0.443	0.0078	3.5
30%—40%	0.440	0.0118	2.8
40%—50%	0.430	0.0200	2.2

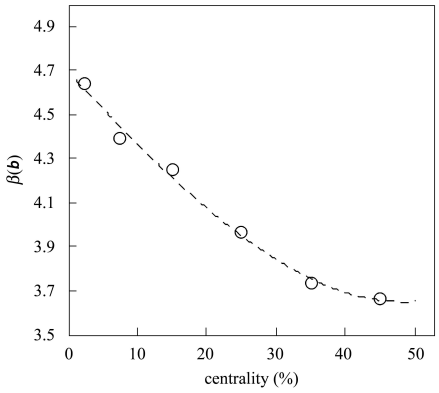

Fig. 6. The relation between $\beta(\boldsymbol{b})$ and the centrality bin.

4 Conclusions

By using the Glauber model, we calculated the number of participants, spectators and binary nucleon-nucleon collisions. From these numbers, we derive the charged-particle pseudorapidity distributions in nucleus-nucleus collisions. The distributions are divided into two parts. One is from the binary nucleon-nucleon collisions, and the other one is from the spectators. As the distributions are used in the special case of Au+Au collisions at $\sqrt{s_{\rm NN}}$=200 GeV, the fitting conditions to the experimental measurements of the BRAHMS Collaboration are very good in each centrality bin over the entire range of pseudorapidity. The most important characteristics of our model are few in free parameters (only two $\alpha(\boldsymbol{b})$ and $\eta_0(\boldsymbol{b})$), clear in the physical picture and simple in treatment. Furthermore, our model can also be used to describe the charged-particle pseudorapidity distributions in unequal-nucleus collisions.

References

1 SHAO Feng-Lan, YAO Tao, XIE Qu-Bing. Phys. Rev. C, 2007, **75**: 034904
2 Kharzeev D, Nardi M. Phys. Lett. B, 2001, **507**: 121—128
3 Kharzeev D, Levin E. Phys. Lett. B, 2001,**523**: 79—87
4 Capella A, Sousa D. Phys. Lett. B, 2001,**511**: 185—190
5 Eskola K J, Kajantie K, Ruuskanen P V et al. Phys. Lett. B, 2002, **543**: 208—216
6 Back B B, Baker M D, Barton D S et al. Phys. Rev. Lett., 2001, **87**: 102303
7 Back B B, Baker M D, Barton D S et al. Phys. Rev. Lett., 2003, **91**: 052303
8 Adler S S, Afanasiev S, Aidala C et al. Phys. Rev. Lett., 2003,**91**: 072301
9 Bearden I G, Beavis D, Besliu C et al. Phys. Rev. Lett., 2002, **88**: 202301
10 LIU Fu-Hu. Phys. Lett. B, 2004, **583**(1): 68—72
11 MENG Cai-Rong, LI Xiao-Lin, DUAN Mai-Ying. HEP & NP, 2004, **28**(11): 1165—1169 (in Chinese)
12 LIU Fu-Hu, Panebratsev Y A. Nucl. Phys. A, 1998, **641**(4): 379—385
13 LIU Fu-Hu, Panebratsev Y A. Phys. Rev. C, 1999, **59**(2): 1193—1195
14 LIU Fu-Hu, Panebratsev Y A. Phys. Rev. C, 1999, **59**(3): 1798—1801
15 LIU Fu-Hu, YIN Xin-Yi, TIAN Jun-Long et al. Phys. Rev. C, 2004, **69**(3): 034905
16 DONG Ya-Fei, JIANG Zhi-Jin, WANG Zeng-Wei. Chinese Physics C (HEP & NP), 2008, **32**(4): 259—263
17 Glauber R J. Lectures in theoretical physics. Interscience, New York, 1959, **1**: 315
18 WONG Cheuk-Yin. Introduction to Heavy-ion Collisions at High Energy. Haerbin: Haerbin Institute of Technology Press, 2002. 222—230 (in Chinese)
19 Werner K. Phys. Rep., 1993, **232**: 87—299
20 Frois B, Bellicard J B, Cavedon J M et al. Phys. Rev. Lett., 1997, **38**: 152—155
21 Adler C, Ahammed Z, Allgower C et al. Phys. Rev. Lett., 2002, **89**: 202301
22 WONG C Y. Phys. Rev. D, 1984, **30**: 961—971
23 Alner G J, Alpgaord K, Anderer P et al. Phys. Rep., 1987, **154**: 247—383
24 Barshay S. Phys. Rev. D, 1984, **29**: 1010—1012
25 Pajares C, Ramallo A V. Phys. Rev. Lett., 1984, **52**: 407—409
26 Adler S S, Afanasiev S, Aidala C et al. Phys. Rev. C, 2004, **69**: 034909
27 Back B B, Baker M D, Barton D S et al. Phys. Rev. C, 2005, **72**: 031901